

# Exploring the key facets of leakage dynamics in water distribution networks: Experimental verification, hydraulic modeling, and sensitivity analysis

Dina Zaman<sup>a</sup>, Ashok Kumar Gupta<sup>b,\*</sup>, Venkatesh Uddameri<sup>c</sup>, Manoj Kumar Tiwari<sup>a</sup>, Dhrubajyoti Sen<sup>b</sup>

<sup>a</sup> School of Water Resources, Indian Institute of Technology Kharagpur, Kharagpur, 721302, India

<sup>b</sup> Department of Civil Engineering, Indian Institute of Technology Kharagpur, Kharagpur, 721302, India

<sup>c</sup> Department of Civil, Environmental, and Construction Engineering, Texas Tech University, Lubbock, TX, 79409-1023, USA

## ARTICLE INFO

Handling Editor: Mingzhou Jin

Keywords:  
EPANET 2.0  
Calibration  
Pipe roughness  
Emitter coefficient  
Emitter exponent  
Sensitivity analysis

## ABSTRACT

Hydraulic solvers are extensively used for the real-time operational analysis and asset management of water distribution networks. However, the influence of leakage on network hydraulics is still not fully understood, and limited experimental verification concerning leakage modeling and calibration efficacy of hydraulic solvers is presently available. To address these limitations, this research develops a novel strategy to quantitatively assess the efficacy of the popular hydraulic solver, EPANET 2.0 in emulating the leakage dynamics through an extensive experimental study conducted on a realistic sensor-equipped network prototype followed by comprehensive leakage modeling and analysis. The network response to diverse leak scenarios is experimentally analyzed, and the inferences derived are utilized to configure the leak models. A stage-wise calibration routine of the base and leak models is executed, which exhibits reasonable accuracy with mean absolute errors of 0.011 and 0.060, respectively. The calibrated leak models manifest satisfactory performance concerning the simulated system pressure and effectively predict the leak flow trends at all leakage levels. The sensitivity matrix of the leak models also captures the variation in the localized and global impact of leak levels on system flow and pressure concerning different leak scenarios. Thus, this research experimentally verifies the efficacy of leakage modeling using EPANET 2.0 and delineates the potential challenges concerning efficient calibration and performance analysis of leak models using the predefined leak parameters. The implications of this study can be instrumental for utility managers and researchers in configuring improved leak models using hydraulic solvers and strategizing model-based leakage management plans.

## 1. Introduction and state-of-the-art

Water supply systems are recognized as critical urban infrastructures of high socio-economic value amidst water scarcity, resource insufficiency, and climate change stresses (Garnier and Holman, 2019; Ji et al., 2020). While centralized water treatment plants are responsible for the production of safe and affordable drinking water, the efficient conveyance of the treated water to the prospective consumers through water distribution networks (WDNs) plays an equally important role in ensuring the environmental and financial sustainability of these centrally managed water infrastructure (Salomons and Housh, 2020). WDNs serve as the arterial system of any city and entail a huge

establishment cost, along with tremendous energy and manpower resources for its continuous operation and maintenance (Dave and Layton, 2020). Efficient management of WDNs is paramount to maintaining optimal hydraulic performance while minimizing water losses, in-route contamination, and energy consumption in these systems (Bonthuys et al., 2019).

Real-time operational analysis and asset management of WDNs is rather improbable using analytical techniques, and hydraulic simulators/solvers are extensively used for these purposes (Chu et al., 2020). Hydraulic modeling and simulation of large WDNs is a challenging and data-intensive process that requires efficient model calibration and experienced performance interpretation by skilled personnel to account for the non-linear and multi-parametric nature of these systems (Hu

\* Corresponding author.

E-mail address: [agupta@civil.iitkgp.ac.in](mailto:agupta@civil.iitkgp.ac.in) (A.K. Gupta).

<b>List of abbreviations</b>	
<b>Acronyms</b>	
WDNs	Water distribution networks
EPANET	Environmental Protection Agency NETwork
GI	Galvanized Iron
RMSE	Root Mean Square Error
SCADA	Supervisory Control And Data Acquisition
HMI	Human-Machine Interface
ADC	Analog/Digital Convertor
PLC	Programmable Logic Controller
US	Upper section
MS	Middle section
DS	Downward section
IF	Inflow meter
OF	Outflow meter
PM	Pressure monitoring nodes
<i>Parameters/Notations</i>	
$Q_L$	Leak flow rate
$A_L$	Area of leakage
$C_d$	Coefficient of discharge
$g$	Gravitational constant
$P$	System pressure/nodal pressure
$k$	Emitter coefficient
$e$	Emitter exponent
$N_L$	Leakage number
$C$	Hazen-Williams coefficient
L1 to L4	Leakage levels
N	No. of pressure monitors
$P_{EXP}$	Observed pressures
$P_{SIM}$	Simulated pressures
$C$	Hazen-Williams coefficient
$C_{OPT}$	Optimal C value
$[k, e]_{OPT}$	Optimized leak parameters
$q$	Pipe flow
$h$	Pipe headloss
$d$	Pipe diameter
$L$	Length of the network pipe
$Q$	Nodal flow

et al., 2021). Along with the structural and operational complexities, the uncertainties associated with estimating network parameters such as nodal demand, pipe roughness, pipe diameter, and valve status pose a significant challenge to WDN modeling, calibration, and analysis (Seifollahi-Aghmuni et al., 2013).

One of the key factors that jeopardize the structural integrity and functional capacity of WDNs is the occurrence of pipe failure and leakage (Sanjuan-Delmás et al., 2015). Leakage in WDNs largely remains unnoticed, leading to the progressive deterioration of hydraulic performance and in-route contamination of treated water (Zaman et al., 2021a). It further increases the scope of parametric uncertainty in terms of leak location, size, shape, and loss flow rate in WDNs (Zaman et al., 2020) that needs to be accounted for during hydraulic modeling and calibration (Koppel and Vassiljev, 2012). Appropriate leakage modeling is also essential to obtain the localized and global impact of leaks on the network hydraulics while conducting model-based studies for planning leakage management actions (Berardi and Giustolisi, 2021).

Incorporating leakage dynamics in network analysis and performance assessment is crucial for the realistic approximation of the WDN behavior (Zaman et al., 2021b). From the modeling perspective, leakage in WDNs behaves as an additional and unpaid demand volume, resulting in an immediate pressure reduction in its vicinity and a cumulative increase in the overall water and energy losses (Zaman et al., 2021a). Understanding the leak implications on network hydraulics has received significant research focus in the past two decades, and diverse standpoints concerning leakage modeling and simulation, intrinsic leak behavior, and leak response in the real field have been investigated.

### 1.1. Water loss estimation and leakage modeling

Water utility managers utilize several leak-related indicators/indices such as non-revenue water, leakage per meter, leakage per connection, and infrastructure leak index for water loss estimation in real WDNs (Zaman et al., 2020). Although fairly useful for quantifying the overall water loss in real-field systems, most of these indices are system-specific and do not provide adequate insight into the characteristic leakage dynamics and WDN performance efficiency (Zaman et al., 2021b).

Leakage modeling and simulation are crucial for various studies conducted in the realm of model-based approaches of WDN management (Fuchs-Hanusch et al., 2016). Leakage is simulated as a pressure-driven phenomenon using the generalized form of the orifice

equation or Torricelli's formula ( $Q_L = A_L C_d \sqrt{2gP}$ ), as depicted in Eq. (1) (Fox et al., 2017).

$$Q_L = k P^e \quad (1)$$

Here,  $Q_L$  is the leak flow rate (L/s),  $A_L$  is the area of leakage,  $C_d$  is the coefficient of discharge,  $g$  is the gravitational constant,  $k$  is the emitter coefficient,  $P$  is the pressure head (m), and  $e$  is the emitter exponent.

When compared to the orifice equation,  $k$  is equivalent to the area of leakage ( $A_L$ )  $\times$  discharge coefficient ( $C_d \times \sqrt{2g}$ ) and is also denoted as the 'effective leak area' (Fuchs-Hanusch et al., 2016). Ferrante (2012) experimentally established that elastically deforming pipes exhibit linear variation of  $k$  with pressure, whereas non-linear relationship becomes evident for viscoelastic and elastoplastic pipe material. The change in  $A_L$  was experimentally observed to impose a more dominant influence on the overall leakage dynamics compared to  $C_d$  (Fox et al., 2017).

The value of  $e$  is equal to 0.5 for the orifice equation, which denotes only circular openings/leaks. In real-field systems, the value of  $e$  depends on the pipe material and failure modes and governs the pressure sensitivity of the leak flow rates (Fox et al., 2017). Friedl et al. (2012) investigated the propensity of different pipes to undergo material-specific leak failure. They observed that cast iron pipes are prone to experience all failure types, while corrosion pitting is the most common cause of leakage in steel and ductile iron pipes, and plastic pipes mostly suffer from longitudinal cracks. From an extensive literature survey of emitter exponents derived from field and experimental investigations, Fuchs-Hanusch et al. (2016) reported that the values of  $e$  may vary over a wide range from values as low as 0.36 and even as high as 2.5, depending on the pipe materials and failure modes.

### 1.2. Leak response to network hydraulics

The influence of intrinsic and extrinsic factors such as pipe material and system pressure on leakage response in pressurized pipes has been determined through various numerical and experimental studies. Finite element analysis was utilized to establish that the impact of system pressure on the leak area was the lowest for circular openings, followed by circumferential and longitudinal leak openings (Cassa et al., 2010). It also indicated that the effect of longitudinal pipe stresses was higher in circular and circumferential cracks, compared to longitudinal failure. Ssozi et al. (2016) numerically investigated the effect of viscoelastic

behavior in different plastic pipes subjected to round and longitudinal leaks and quantified the instantaneous elastic deformation followed by time-dependent creep response with pressure. Schwaller and van Zyl (2015) analyzed the sensitivity of the emitter exponent,  $e$  of a leak model to the parametric variations in a hypothetical network and estimated that mean system pressure had the highest impact on emitter exponent, followed by leak area and system pressure range.

Experimental studies on the intrinsic leakage behavior for different pipe properties and pressure conditions were conducted by Fox et al. (2017) to understand longitudinal leaks' response in viscoelastic pipes. The study concluded that material strain and leak area are intricately related and verified the suitability of the orifice equation in modeling the dynamic leak flow rates from longitudinal slits with accurate incorporation of the leak area. Cassa and van Zyl (2014) introduced a novel dimensionless constant, Leakage Number ( $N_L$ ), to describe the variation in leakage exponent with system pressure for elastically deforming leaks in pressurized pipes. This study was further extended to numerically establish the applicability of the theoretical pressure-leak relationship for individual leaks in explaining the actual leak response encountered in the field by Schwaller and van Zyl (2015).

### 1.3. WDN modeling and calibration

Several public domain hydraulic network solvers such as EPANET, Branch, and LOOP, along with commercial software packages such as WaterCAD, WaterGEMS, InfoWorks WS, are presently used for real-time analysis of WDNs (Zaman et al., 2020). Among these, EPANET, developed by the United States Environmental Protection Agency (U.S. EPA), is arguably the most popular network solver for WDN modeling and analysis (Rossman, 2000). Most urban water utilities worldwide utilize the EPANET platform in some capacity for designing, analyzing, or optimizing their network operations (Bonthuys et al., 2019). Moreover, the dynamic linking of the EPANET object library enables its interfacing with programming and numeric computing platforms such as R (Eck, 2016), MATLAB (Eliades et al., 2016), and Python (Steffelbauer and Fuchs-Hanusch, 2015) for carrying out advanced hydraulic analysis, which has been immensely useful in research.

Seifollahi-Aghmuni et al. (2013) assessed the impact of pipe roughness uncertainty on the overall network performance and computed the probabilistic roughness series, using EPANET 2.0 and Monte Carlo simulations (MCS) to estimate the optimal operation period of WDNs. Hydraulic modeling in EPANET to incorporate pressure-driven analysis was also extensively studied by several researchers (Jun and Guoping, 2013). Sensitivity analysis of the WDN response to the parametric uncertainty was initiated by Nian-dong et al. (2017) and its application in leakage assessment using EPANET was proposed by Geng et al. (2019).

EPANET has been extensively used as a research tool for model-based studies on standard numerical WDN models such as Anytown (Zaman et al., 2021b), Apulian (Jun and Guoping, 2013), or real network models (Cavazzini et al., 2020). Such model-based studies necessitate the utilization of a well-calibrated WDN model, which is a major challenge. Although modeling platforms are seldom expected to truly emulate real hydraulic and leakage responses, a reasonable consistency of the simulated state variables with the observed parameters is essential for model-based analyses (Vrachimis et al., 2021). Several WDN model calibration protocols considering different network parameters, such as system demand (Chu et al., 2020) and pipe roughness properties (Koppel and Vassiljev, 2009) have been proposed. Sanz and Pérez (2015) presented a demand calibration methodology by utilizing Singular Value Decomposition of the sensitivity matrix to solve the optimization problem. Sophocleous et al. (2017) proposed a model calibration procedure coupled with leak detection in a two-stage process using genetic algorithms to solve the optimization problem.

### 1.4. Research goals and objectives

The extensive survey on various aspects of leakage dynamics in WDN modeling revealed significant knowledge gaps in the existing literature. Although experimental investigations have adequately demonstrated the leakage modeling efficacy of the modified orifice equation using single-pipe systems, their applicability in representing the interaction between structural and leakage dynamics in full-scale WDN models has not been fully understood. Despite the widespread use of hydraulic solvers such as EPANET 2.0 for WDN simulation and analysis, limited studies have experimentally investigated and verified the leakage modeling efficacy of these software platforms in emulating real-time operational behavior. Existing studies have inadequately explored the challenges of model calibration considering the leak-induced factors in real WDN models, which is another major research gap.

The specific research questions that summarize the identified research gaps and align the major objectives of this study are enumerated below.

- How effective are the hydraulic modeling platforms in emulating the real-time operational behavior of WDNs considering system leakage?
- What is the impact of leak-induced factors on the simulated outcomes in WDN models?
- How efficiently can system leakage be modeled and calibrated using the predefined leak parameters?
- What is the localized versus global sensitivity of the simulated state variables for diverse leakage conditions?

The primary aim of this study is to address these research questions for which extensive leak experiments were conducted on a newly fabricated network prototype equipped with flow and pressure monitoring sensors and a hydraulic model of the experimental network was configured using EPANET 2.0. The inferences derived from the experimental results were used to quantitatively verify the efficacy of the hydraulically simulated outcomes in EPANET 2.0 for leak-induced conditions through the stage-wise calibration of base and leak models (Rossman, 2000). The performance of the calibrated leak models were verified for the simulated pressure and leak flow rates concerning the predefined leak parameters. The sensitivity of the state variables of the simulated network to the diverse leak scenarios was ascertained through the analytical solution of the Jacobian matrices. The generalized framework developed for integrated leakage modeling, calibration, and sensitivity analysis of real WDN models can be instrumental in configuring improved leakage models and analyzing the effectiveness of model-based leakage management strategies, which is the novel contribution of this study.

## 2. Materials and methods

### 2.1. Experimental set-up

A relatively complex grid-type experimental network prototype (15 m × 12 m) was designed and fabricated in the laboratory for conducting controlled leakage experiments for different hydraulic conditions. The experimental facility consisted of 37 network nodes, 61 Galvanized Iron (GI) pipe sections of 100 mm, 80 mm, or 50 mm diameter with a total pipe length of 147 m. An overhead tank and inlet pump arrangement was provided for continuous water supply to the network during experimentation. The network was equipped with ten pressure transmitters, an inflow rate sensor (electromagnetic flowmeter) located at the network inlet, and outflow rate sensors (electromagnetic and paddle-wheel flowmeters) located at the network outlets signifying demand locations. Valve actuators with variable opening provisions were attached to the pipe sections to regulate leaks of increasing flow rates at different locations. Fig. 1 illustrates (a) the actual experimental network and (b) the schematic layout portraying the strategic sensor placement

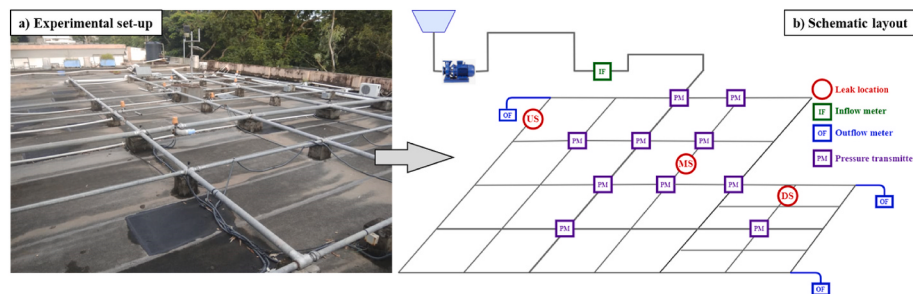


**Fig. 1.** a. Laboratory-scale experimental network for controlled leakage experimentation, b. Schematic layout with salient network components (US – upper section, MS – middle section, DS – downward section).

and leak-simulation locations.

Similar to real-world WDNs, the network was equipped with a supervisory control and data acquisition (SCADA) system for real-time monitoring, control, and data logging during experimental operations. Further information on the sensing and control equipment used in the experimental network is presented in Section S1 of Supplementary Information (SI). The inlet pump and the leak-simulating actuators were remotely controlled through the Human Machine Interface (HMI) panel to initiate and terminate the network operations and maneuver the valve openings to generate the leak events of different flow rates. The real-time analog data monitored through the flow sensors and pressure transmitters were digitized by the Analog/Digital Converter (ADC) in the Programmable Logic Controller (PLC) and visualized in the HMI panel. Data was logged at a 1-s interval during experimental operation and stored in the SCADA repository. Fig. 2 presents the key components of the SCADA architecture in connection to the experimental operation.

A full-fledged quality assurance and control routine was undertaken to confirm the network's fitness for leak experimentation. Trial tests were conducted to identify the faulty pipe joints that generated background leaks and rectify them. The pressure transmitters were calibrated at three levels (0%, 50%, and 100%) for a 4–20 mA output range and compared with the reference pressure. The inflow sensor (electromagnetic flowmeter) was physically verified at different flow volumes to ensure that correct response and consistent data output from the flow sensor was obtained. The flow logged in the outflow rate sensors (paddlewheel flow meters) was individually verified concerning the inflow sensor, and the corresponding instrumental bias was determined for

each flowmeter. The final calibrated network was operated for a substantially long period, and the quasi-steady-state behavior of the network was analyzed using the time-series data. Based on the outcomes, the network was operated for at least 3000 s before introducing leak events and the data collected for the initial 500 s of baseline experiments were discarded to eliminate the effects of transient behavior.

## 2.2. Experimental design for data acquisition

An experimental strategy with multi-pressure and multi-flow conditions was designed for this study, incorporating the different aspects of the real-time WDN operation. For each experiment, the network was operated under normal conditions with the specified demand nodes open at an initial outflow rate of  $\sim 27 \text{ m}^3/\text{h}$  and all leak valves closed for a period  $\sim 3000 \text{ s}$  before introducing leaks. Three leak locations situated at the upper section (US), middle section (MS), and downward section (DS) concerning the network inlet were identified for leak experiments. Experiments at the base level (L0 – no leak) and four leakage levels (L1, L2, L3, and L4) with increasing leak flow rates (or leak flow area) were sequentially simulated at the leak locations (US, MS, DS) for a period of 100 s each by maneuvering the valve opening to 0, 12, 24, 36, and 48%, respectively. The leak flow rates induced during the experiments were intentionally kept high so that their impact on the network hydraulics was explicitly captured, overcoming the system randomness and associated noise. The remotely monitored flow rates at the inflow meter (IF), outflow meter (OF), and the pressure in the ten pressure monitoring nodes (PM) were retrieved from the SCADA repository as time-series

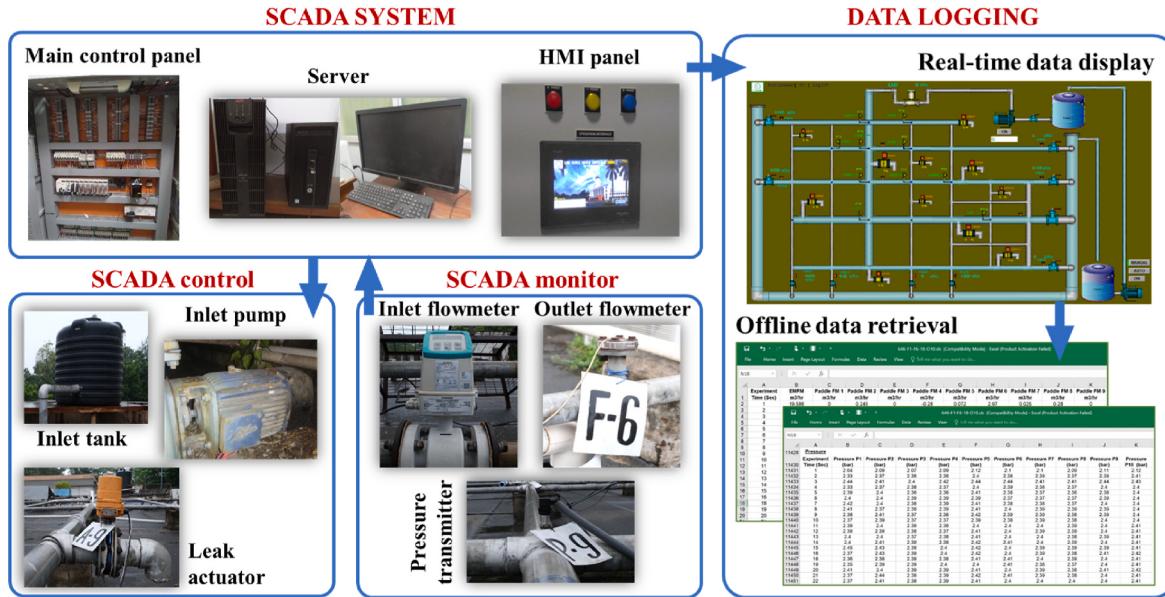


**Fig. 2.** Monitoring, control, and data logging facilities of the SCADA system concerning the experimental network.

data in excel file formats and a preliminary data cleaning process was conducted to substitute the missing values and exclude the initial transient data.

### 2.3. Hydraulic modeling and calibration in EPANET 2.0

A demand-driven analysis approach was implemented for hydraulic simulation in EPANET 2.0, while leak simulation was executed through pressure-driven analysis. Leakage was hydraulically modeled using Eq. (1), wherein the emitter exponent,  $e$ , was configured as a global parameter and emitter coefficient,  $k$ , was set as a localized parameter on the concerned leak node of the WDN model. The  $e$  value was fixed at 0.5 in the default settings of EPANET 2.0. The results obtained through the controlled base and leak experiments were utilized to configure the best possible configuration of the base and leak models for model performance assessment. A stage-wise implicit calibration procedure for the base and leak models was implemented by coupling the EPANET programmers' toolkit with MATLAB 2019b (Eliades et al., 2016).

The base model was configured with known experimental outflow rates in the demand locations. Since the network is newly built, it is assumed that there are no incrustations in the network pipes. Pipe roughness denoted by Hazen-Williams coefficient ( $C$ ) was assumed as the only unknown parameter, and the base model was calibrated by solving the inverse optimization problem. For each candidate  $C$  value, the minimum error function concerning the observed ( $P_{EXP}$ ) and simulated pressures ( $P_{SIM}$ ) at  $N$  pressure monitoring locations were formulated to determine the optimal  $C$  value ( $C_{OPT}$ ), as depicted in Eq. (2).

$$f(C_{OPT}) = \min \sqrt{\frac{1}{N} \sum_{i=1}^N [P_{EXP} - P_{SIM}(C)]^2} \quad (2)$$

Subject to:  $120 \geq C \geq 60$

Subsequently, the calibrated base model with the  $C_{OPT}$  value was used to prepare the leak models for different leak scenarios. The reduced outflow rates at the demand nodes were estimated from experimental analysis and incorporated in the corresponding leak models. The leak models were calibrated considering the leak parameters -  $k$  and  $e$  as the unknown parameters by solving the inverse optimization problem. For each candidate pair of leak parameters  $[k, e]$ , the minimum error function concerning the observed ( $P_{EXP}$ ) and simulated pressure ( $P_{SIM}$ ) outcomes at  $N$  pressure monitoring locations were formulated as depicted in Eq. (3) to determine the optimized leak parameters  $[k, e]_{OPT}$ , corresponding to each leak model.

$$f([k, e]_{OPT}) = \min \sqrt{\frac{1}{N} \sum_{i=1}^N [P_{EXP} - P_{SIM}(k, e)]^2} \quad (3)$$

Subject to:  $\begin{cases} C = C_{OPT} \\ 0.1 \leq k \leq 3.0 \\ 0.1 \leq e \leq 3.0 \end{cases}$

### 2.4. Leak sensitivity analysis

The localized and global sensitivity of the simulated state variables for diverse leakage conditions was obtained for the calibrated base and leak models. The sensitivity of the nodal pressure to the nodal flow for 'no leak' and 'leak' conditions was estimated using the matrix analysis method for deducing the analytical solution of the Jacobian matrix of each model (Nian-dong et al., 2017). The incidence matrix ( $A_{n \times m}$ ) describing the topological information of the WDN with  $n$  nodes and  $m$  pipes is given by Eq. (4) (Nian-dong et al., 2017).

$$A_{n \times m} = \begin{cases} -1 & \text{if node } n \text{ is the start node to pipe } m \\ 0 & \text{if node } n \text{ is not connected to pipe } m \\ +1 & \text{if node } n \text{ is the end node to pipe } m \end{cases} \quad (4)$$

Denoting the Hazen-Williams equation for computing pipe headloss in the form of Eq. (5), the partial differential equations for the network pipes of length ( $L$ ) concerning the pipe flow ( $q$ ) to the pipe headloss ( $h$ ) were computed (Nian-dong et al., 2017).

$$q = C \left( \frac{hd^{4.871}}{L} \right)^{\frac{1}{1.852}} \quad (5)$$

The binary vectors deduced for the network pipes were used to configure the diagonal matrix,  $B_{m \times m}$  as depicted in Eq. (6) (Nian-dong et al., 2017).

$$B_{m \times m} = \begin{bmatrix} \frac{\partial q_1}{\partial h_1} & & & \\ & \frac{\partial q_2}{\partial h_2} & & \\ & & \ddots & \\ & & & \frac{\partial q_m}{\partial h_m} \end{bmatrix} \quad (6)$$

The sensitivity matrix (Jacobians) of the nodal flow ( $Q$ ) to nodal pressure ( $P$ ) and pipe flow ( $q$ ) was obtained, as described in Eq. (7) (Nian-dong et al., 2017).

$$\begin{cases} \frac{\partial P}{\partial Q} = -(ABA^T)^{-1} \\ \frac{\partial q}{\partial Q} = BA^T(ABA^T)^{-1} \end{cases} \quad (7)$$

## 3. Results and discussion

### 3.1. Experimental study

#### 3.1.1. Visualization and graphical analysis

The experimental data retrieved from the SCADA repository were graphically analyzed to determine the impact of diverse leak scenarios on the state variables. The continuous inflow rate, total outflow rate, and pressure signals were extracted for 500 s to include base and leak experiments conducted at the US, MS, and DS locations, and the respective time-series statistics are depicted in Fig. 3. The impact of leakage levels (i.e., increase in leak flow rates) was manifested in the system inflow rate, outflow rates, and pressure. However, the impact of leak location on the deviation in state variables was not discernible from the time series plots on an equivalent scale, which necessitated further detailed investigation.

A delineated illustration of the leak experiments at the US location and an enlarged view of a single leakage level (L1) is depicted in Fig. 4. The accelerated deterioration of the flow variables (inflow rate and outflow rate) was evident for the increasing leakage levels (L0, L1, L2, L3, L4). Each leakage level generated a transitional effect for  $\sim 20$  s, after which it depicted a nearly steady behavior at a higher inflow rate and lower outflow rate, and their difference indicated the leak flow rate ( $q_{L1}$ ) generated at the specific leak location (Fig. 4a [inset]). An abrupt drop in the network pressure ( $p_{L1}$ ) at all pressure transmitters was captured immediately within  $\sim 5$  s of the leak event (Fig. 4b [inset]). However, pressure signals from the ten transmitters varied within a close band with substantial overlap among the corresponding plots.

#### 3.1.2. Hydraulic response to leak scenarios

The quantitative impact of different leak scenarios on the state variables was ascertained from the experimental data. The flow in the three outlet nodes was combined to obtain the total outflow ( $Q_{OUT}$ ) of the network, while the system pressure ( $P_{AVG}$ ) was computed by averaging the signals in the ten pressure transmitters for the base and leak models. Each leakage level caused an increase in the inflow rate,  $(Q_{IN})_L$  a decrease in the outflow rate  $(Q_{OUT})_L$ , and system pressure  $(P_{AVG})_L$  in the leak models. The percentage variation in the state variables due to

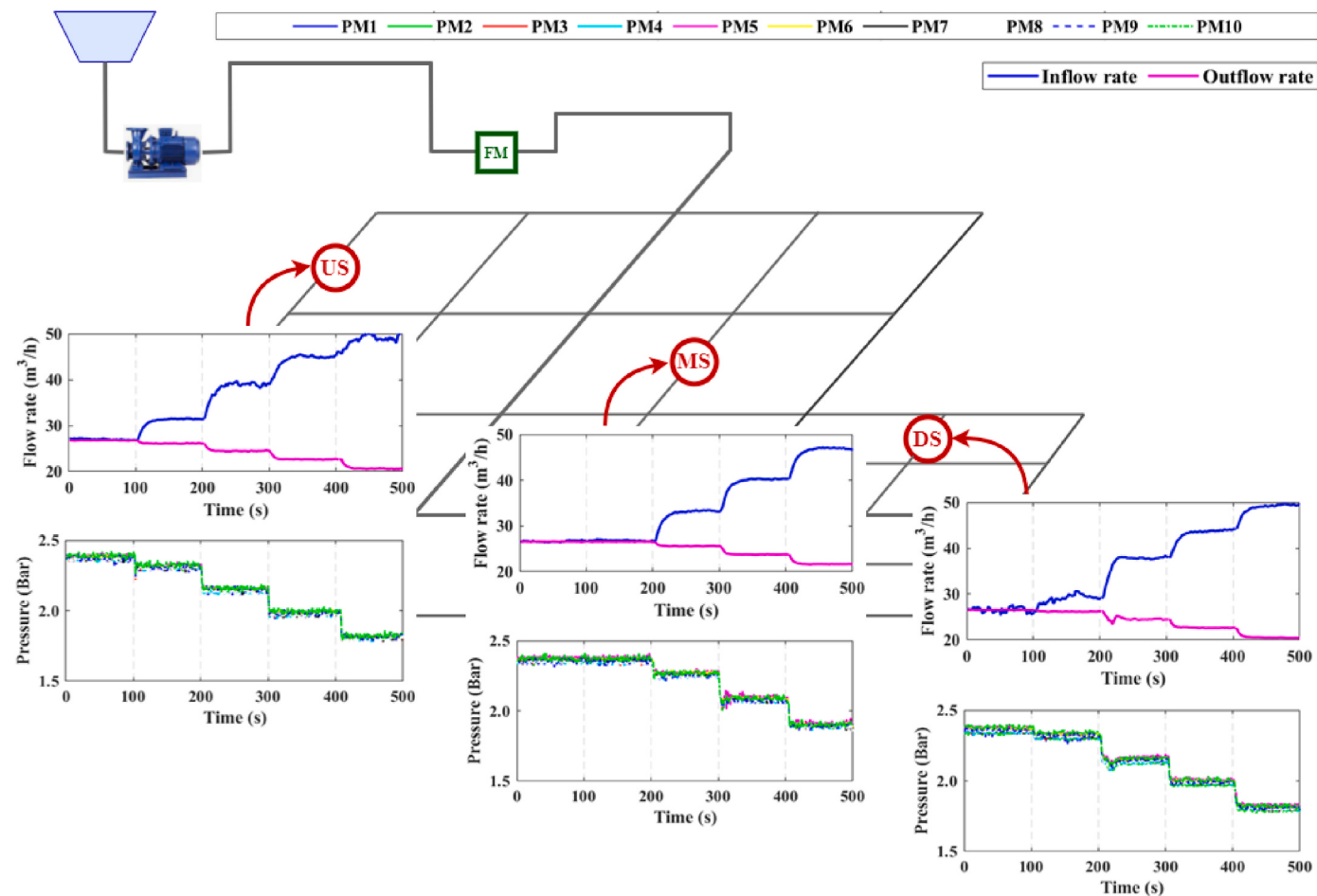


**Fig. 3.** Time-series plots of flow and pressure signals for the base and leak experiments at the US, MS, and DS leak locations (US – upper section, MS – middle section, DS – downward section).

leakage levels ( $L_1, L_2, L_3, L_4$ ) compared to the base level ( $L_0$ ) was computed for the leak models, as presented in Table 1. It was observed that the deteriorative impacts of leakage levels (i.e. increase in leak flow rates) were most discernible on  $(Q_{IN})_L$ , followed by  $(P_{AVG})_L$  and  $(Q_{OUT})_L$ , at all leak locations. The impact of leak was the most significant on the US, followed by DS, and MS for an equivalent leakage level.

The leak flow rate ( $q_L$ ) for leakage level,  $i$  at leak location,  $j$  was computed from the experimental data using Eq. (8).

$$q_{L_{ij}}(\%) = \left[ \frac{(Q_{IN})_{L_{ij}} - (Q_{OUT})_{L_{ij}}}{(Q_{IN})_{L_{ij}}} \right] \times 100 \quad (8)$$

It is deemed more convenient to evaluate the impact of the increasing leak flow rates on the network hydraulics concerning the base or ‘no leak’ scenario ( $L_0$ ). The drop in  $(Q_{OUT})_L$  and  $(P_{AVG})_L$  due to the leakage was assessed concerning the  $Q_{OUT}$  and  $P_{AVG}$  of the base scenario and depicted in Fig. 5. For equivalent leakage levels, the water loss flow rate through the leaks was the lowest at MS location, followed by DS and US location. Presumably, the closer proximity of the US and DS leak nodes to the demand outlets caused the higher leak flow rates in these locations. The MS leak location was remotely located from all demand outlets, perhaps resulting in lower losses for equivalent hydraulic and leakage conditions. The drop in  $(Q_{OUT})_L$  and  $(P_{AVG})_L$  due to leakage was lowest at the MS location and the deviation in the leak flow rates across different leak locations was more apparent at lower leakage levels than higher ones.

### 3.2. Model calibration

#### 3.2.1. Base model calibration

The experimental network was operated under ‘no leak’ condition with the demand nodes delivering a total outflow rate of  $\sim 27 \text{ m}^3/\text{h}$ , and three time-series data of the state variables were registered for  $\sim 3000 \text{ s}$  each. The parameters of the base model were set up assuming a newly built network with negligible structural deterioration. The average outflow rates ( $Q_{OUT}$ ) obtained from the experimental results were used for demand flow rate modeling, and the simulated pressures at the ten pressure monitoring locations (PM1–10) were used for pipe roughness (C) calibration. The base model was iteratively calibrated for C values ranging from 120 to 60 to minimize the objective function described in Eq. (2) and the results obtained are depicted in Fig. 6. The lowest RMSE of  $0.14 \pm 0.01$  was attained for the C value of 75 and the corresponding observed and simulated pressures at the ten pressure monitoring locations (PM1–10) are depicted in Fig. 6 [inset]. The base model upon calibration exhibited a maximum error of 0.019 and a mean absolute error was 0.011 between the observed and simulated pressures.

#### 3.2.2. Leak model calibration

The calibrated base model ( $C_{OPT} = 75$ ) was used to configure the leak models by superimposing a leak node corresponding to the experimental US, MS, and DS leak locations, respectively. Since EPANET 2.0 version does not support pressure-driven analysis, the reduced outflow rates experimentally obtained at the leakage levels ( $L_1, L_2, L_3, L_4$ ) was used for demand modeling.

Once the models were configured, an iterative optimization pro-

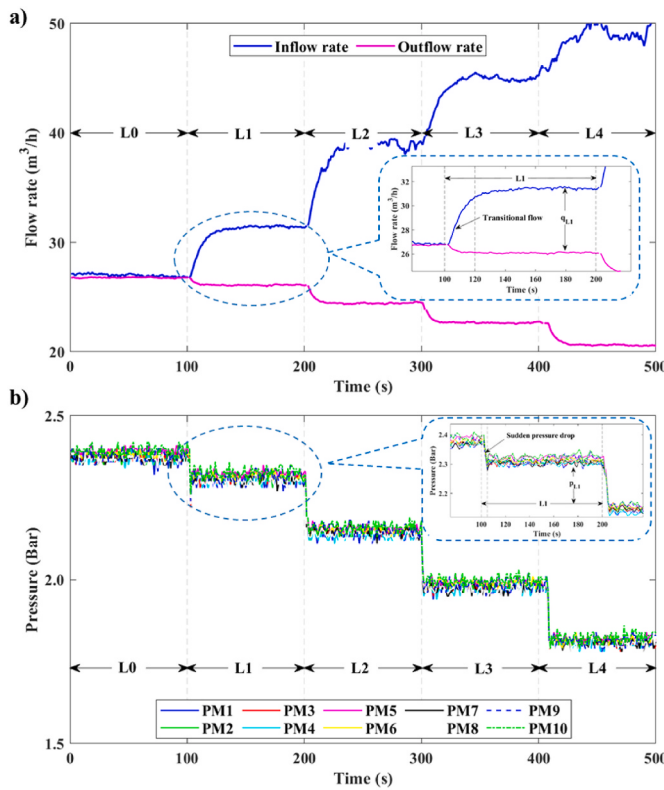


**Fig. 4.** Impact of leaks at the US (upper section) leak location on **a**. Flow rate and **b**. Pressure [(Inset) Enlarged view of the state variables for the leakage level (L1)].

cedure described in Eq. (3) was carried out considering the leak parameters –  $k$  and  $e$ . A wide range of  $k$  and  $e$  values varying from 0.1 to 3.0 was used in the optimization routine to incorporate diverse leak sizes and leak shapes encountered in real networks and the generated response surface of the objective function was obtained for each leak model, as depicted in Fig. 7.

It was evident from Fig. 7 that all leak models demonstrated a large number of local minima, which indicated towards non-uniqueness of the minimized solutions. For each value of emitter coefficient,  $k$  the model predicted a local minimum corresponding to an emitter exponent,  $e$ . The most optimal pair of leak parameters,  $[k, e]_{OPT}$  corresponding to the minimum value of the objective function for each leak scenario, was ascertained, as presented in Table 2. The  $[k, e]_{OPT}$  did not depict any definite pattern across the leakage levels and the leak locations.

Ideally, the value of  $e$  should be similar for the same leakage levels (i.e., leak area) across different leak locations, while the value of  $k$  may vary depending on the system pressure. However, no such trend was observed for the  $[k, e]_{OPT}$  values, although the RMSE values varied within a close range for leaks of same levels across different leak locations, as depicted in Fig. 8. This signifies the potential challenge of modeling and calibrating leakage in EPANET using  $k$  and  $e$ . Thus, the calibration

routine necessitates consideration of the physical interpretation of the leak parameters along with the minimization of the objective function for configuring appropriate leak models.

The overall model performance was ascertained for the optimized leak parameters  $[k, e]_{OPT}$  concerning the calibrated leak models. The simulated pressures and leak flow rates compared to the observed pressure and leak flow rates obtained from the experimental operations are depicted in Fig. 9. Although the simulated models consistently underestimated the leak flow rates, the leak models adequately predicted the system pressure and leak flow trends. In addition, the leak flow rates were quantified more accurately at the higher leakage levels than the lower leakage levels. Furthermore, the maximum error between the observed and simulated leak flow rates was highest for the DS leak location, as the impact of parametric non-linearities and uncertainties within the network could have become more apparent at the downstream section.

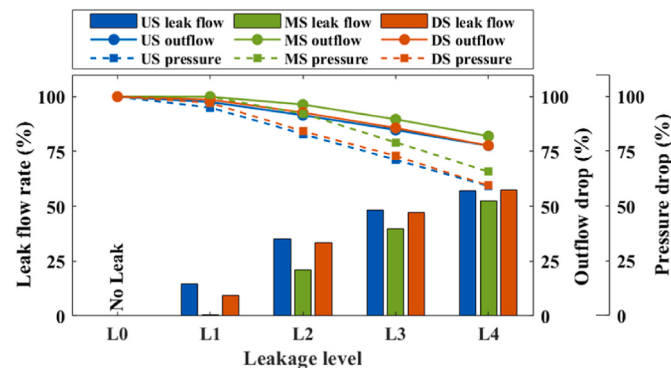


**Fig. 5.** Leak flow rate at leakage levels (L0, L1, L2, L3, L4) across different leak locations and its impact on Outflow drop (%) and Pressure drop (%) (US – upper section, MS – middle section, DS – downward section).

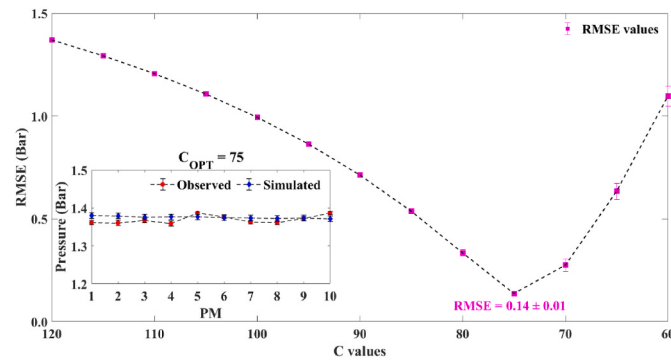


**Fig. 6.** RMSE values for different C values of the base model [(Inset) Observed and simulated pressures at the ten pressure monitoring locations (PM1–10) for the  $C_{OPT} = 75$ ].

**Table 1**

Impact of leak scenarios on the inflow rate ( $(Q_{IN})_L$ ), outflow rate ( $(Q_{OUT})_L$ ), and system pressure ( $(P_{AVG})_L$ ) in the leak models (Here, '+' sign denotes an increase and '-' sign denotes a decrease in the chosen parameter).

	US location			MS location			DS location		
	$(Q_{IN})_L$ (%)	$(Q_{OUT})_L$ (%)	$(P_{AVG})_L$ (%)	$(Q_{IN})_L$ (%)	$(Q_{OUT})_L$ (%)	$(P_{AVG})_L$ (%)	$(Q_{IN})_L$ (%)	$(Q_{OUT})_L$ (%)	$(P_{AVG})_L$ (%)
L0	0	0	0	0	0	0	0	0	0
L1	+14.60	-2.43	-4.93	+0.62	-0.03	-0.06	+9.06	-1.36	-2.85
L2	+41.52	-8.44	-17.05	+21.96	-3.57	-7.73	+39.07	-7.24	-15.74
L3	+64.76	-15.16	-28.75	+48.59	-10.31	-20.79	+62.05	-14.26	-27.00
L4	+80.90	-22.36	-40.74	+73.41	-17.99	-34.14	+83.61	-22.27	-40.52

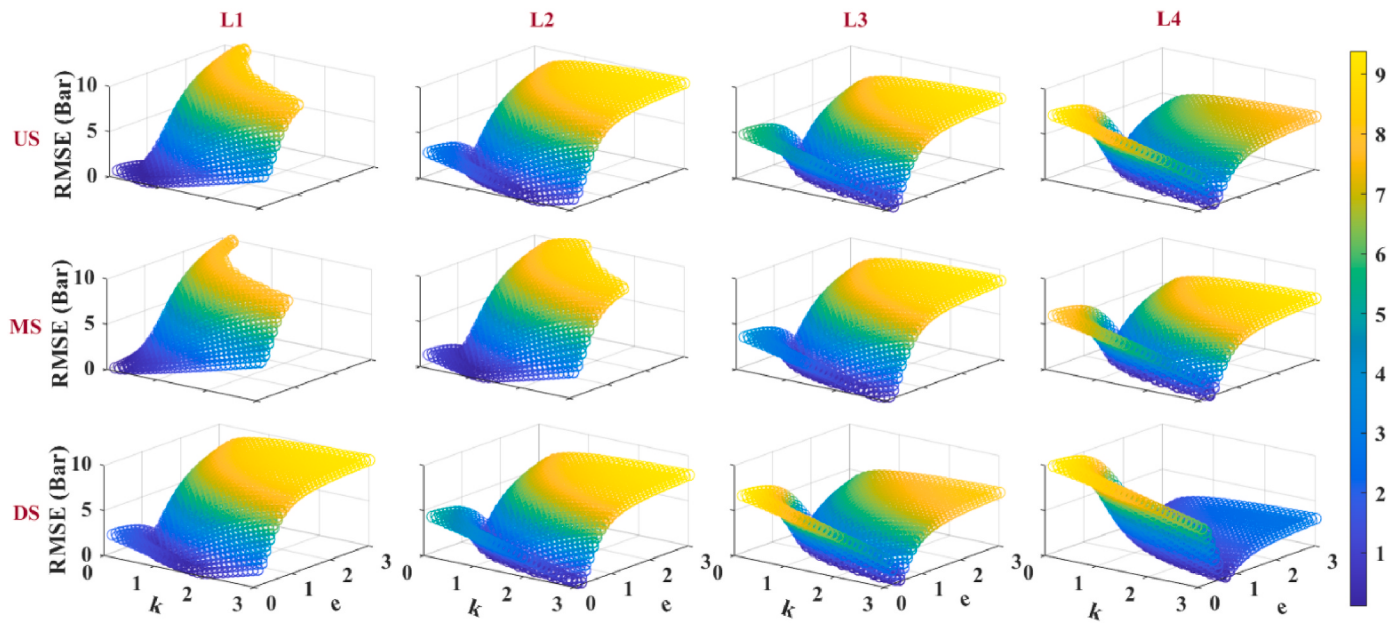


Fig. 7. Response surface of the objective function for the leak models concerning the leak parameters - emitter coefficient ( $k$ ), and emitter exponent ( $e$ ).

**Table 2**  
Optimal leak parameters  $[k, e]_{OPT}$  and corresponding  $RMSE_{MIN}$  values for the leak models.

	US location			MS location			DS location		
	$k$	$e$	$RMSE_{MIN}$	$k$	$e$	$RMSE_{MIN}$	$k$	$e$	$RMSE_{MIN}$
L1	0.20	0.55	0.10	0.10	0.15	0.14	1.8	0.10	0.15
L2	1.55	0.25	0.10	0.10	1.05	0.11	2.85	0.15	0.14
L3	0.60	0.90	0.10	1.35	0.40	0.11	1.90	0.55	0.13
L4	1.70	0.65	0.08	1.50	0.60	0.10	0.50	1.80	0.11

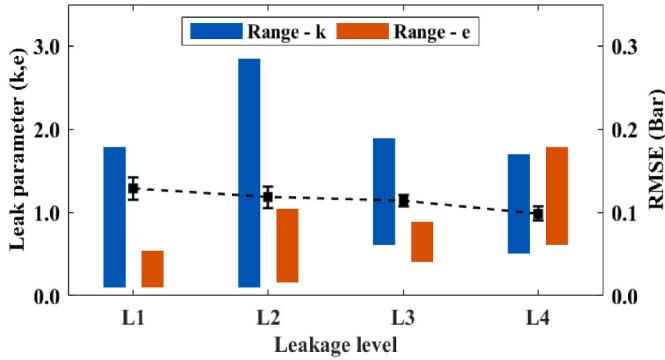


Fig. 8. Range of leak parameters  $[k, e]$  and corresponding  $RMSE_{MIN}$  across the US (upper section), MS (middle section), and DS (downward section) leak locations.

### 3.3. Sensitivity analysis

A sensitivity analysis concerning the base and leak models was conducted to ascertain the impact of leak scenarios on the gradient vectors of network parameters to the state variables. An analytical method for the direct computation of the Jacobian matrices proposed by Nian-dong et al. (2017) was implemented on the hydraulic models using the EPANET-MATLAB programmer's toolkit. The incidence matrix,  $A_{n \times m}$  and diagonal matrix,  $B_{m \times m}$  (not shown here), were constructed for the models using Eqs. (4)–(6). The sensitivity matrix concerning the nodal flow ( $Q$ ) to nodal pressure ( $P$ ) and nodal flow ( $Q$ ) to pipe flow ( $q$ ) was simulated for the leak scenarios using Eq. (7), as depicted in Fig. 10.

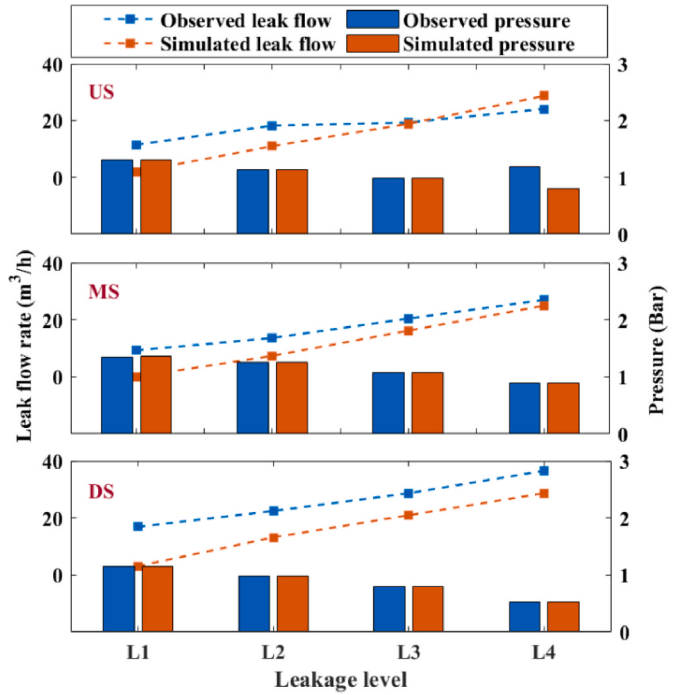
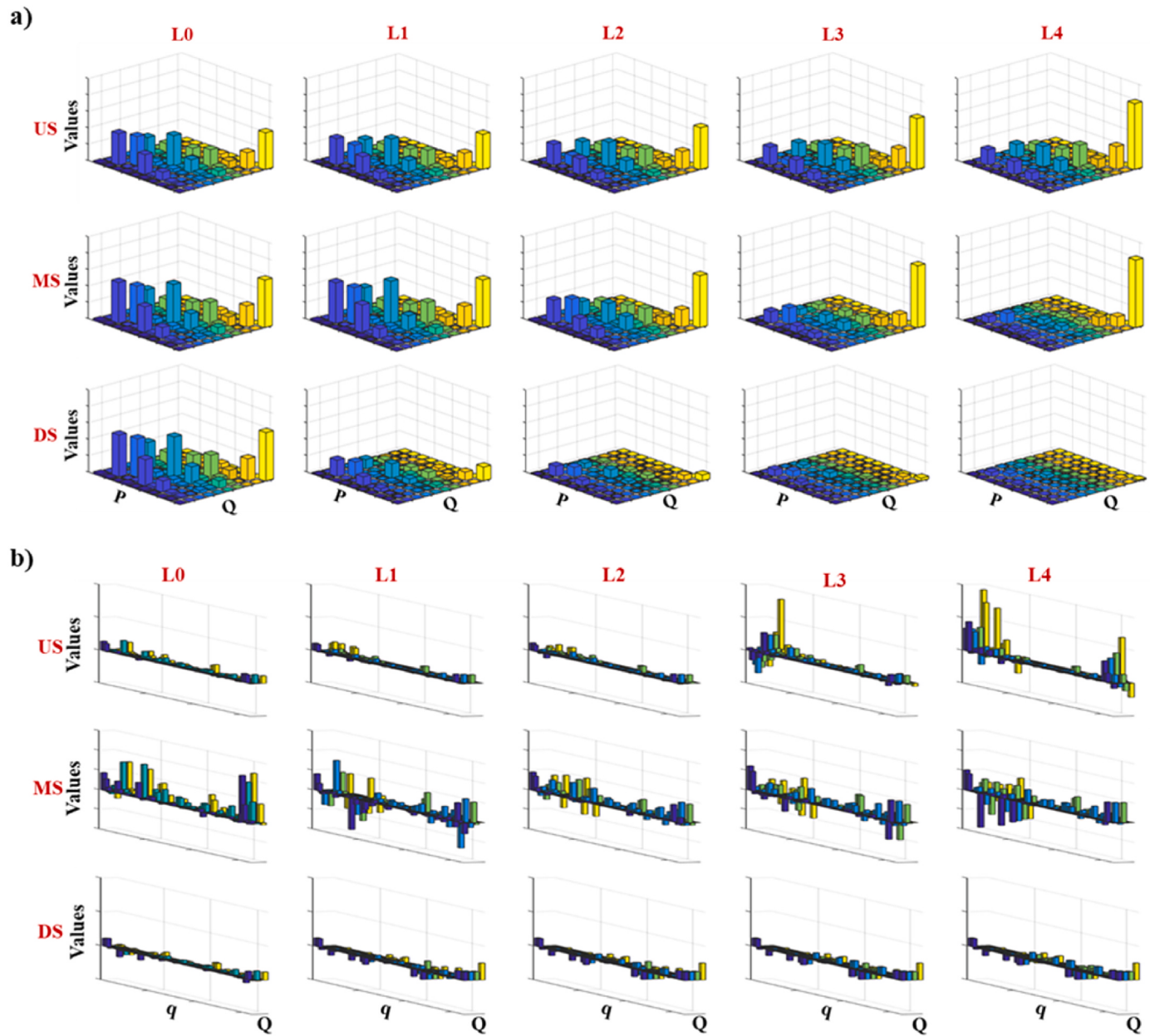


Fig. 9. Performance of the simulated leak models concerning the observed pressure and leak flow rates (US – upper section, MS – middle section, DS – downward section).



**Fig. 10.** Sensitivity matrices concerning the a. nodal flow (Q) to nodal pressure (P), b. nodal flow (Q) to pipe flow (q) for the base (L0) and leak models (L1, L2, L3, L4) at different leak locations (US – upper section, MS – middle section, DS – downward section).

The sensitivity matrix regarding the nodal flow (Q) to nodal pressure (P) at the ten pressure monitoring (PM) locations (Fig. 10a) captured the impact of increasing leakage levels at all leak locations. The sensitivity of the state variables to the leakage levels was lowest at the US leak location, followed by MS and DS locations which signified that leaks caused the highest attenuation of pressure and flow variables when occurring at the downward section of the network. Furthermore, the localized sensitivity of the state variables to the leak scenarios is also discernible from the individual values of the sensitivity matrices. For instance, the PM 10 location depicted the lowest sensitivity to the leakage levels for US and MS leak locations but was highly sensitive to the DS leak location due to its proximity to the leak node.

The sensitivity matrix regarding the nodal flow (Q) to pipe flow (q) for the network pipe sections (Fig. 10b) captured the impact of demand outflow variation, including the loss flow rate in the leak node. The impact of loss flow rates on the pipe flow was highest in the US leak location, followed by MS and DS leak locations, whereas, the pipe flows

at different leakage levels was least sensitive at the DS leak locations. The localized sensitivity of the leak flow rates to the pipe flow was also perceptible at the higher leakage levels.

### 3.4. Discussion

Although hydraulic models of WDNs are immensely useful for utility operators and researchers in conducting diverse model-based network analyses, the influence of leakage dynamics on network hydraulics in a WDN model is still not fully understood. Single pipe systems have adequately emulated the pressure-leak relationship signified by the modified orifice equation, which does not necessarily ensure similar leakage dynamics in real-field systems. As opposed to the considerable number of numerical and experimental studies exploring the pressure-leak relationship in single-pipe systems and rudimentary hypothetical networks, the leakage modeling efficacy of hydraulic solvers has rarely been verified using controlled experimental studies on realistic

networks, which is the main objective of this study. The key inferences derived from the quantitative assessment of leakage behavior in a WDN model can be consolidated into the following major takeaways.

- Leaks in proximity to the demand locations incurred higher leak flow rates and subsequent deterioration of the state variables (inflow rate, system pressure, and outflow rates) than the remotely located leaks, irrespective of their spatial position within the network.
- The leak parameters – emitter coefficient and emitter exponents were rather inadequate in conforming to their physical meaning and emulating the expected hydraulic behavior during leakage but the calibrated leak models exhibited a significant match between the observed and simulated system pressure and leak flow trends, particularly at the higher leakage levels.
- The sensitivity matrix of the calibrated models regarding the nodal flow to nodal pressure and pipe flow adequately captured the impact of leakage levels and leak locations, both at a localized and global scale.
- The stage-wise calibration routine of the base models and leak models is simple, straightforward, and exhibited fairly reasonable performance efficacy concerning the newly fabricated experimental network with nearly uniform pipe roughness.
- A rigorous multi-objective optimization procedure may be more effective for configuring hydraulic models of real-field complex networks by considering pipe roughness and leak parameters as unknown parameters simultaneously. Objective functions can be configured by choosing the boundary conditions (set of feasible alternatives) of each optimizable parameter based on practical experience in the real field.
- While an experimental network was used as a case study, the developed protocol for investigative analysis is inherently model agnostic and can be extended in future work on real-field WDNs. The successful implementation and analysis on controlled leakage scenarios with diverse hydraulic scenarios in a prototype network, in essence, implies the scalability of the proposed methodology to any urban WDN. However, real WDNs trigger more complexities in the hydraulic model leading to higher degrees of freedom that may degrade the calibration efficacy of the leak models.

A conceptual framework synthesizing the key steps of the experimental and data analysis protocol proposed in this study, as depicted in Fig. 11.

#### 4. Conclusions and future research directions

The present study is aimed to provide a unique insight into the performance efficacy of hydraulic models of real WDNs configured and calibrated to account for diverse leak scenarios using the competent hydraulic solver, EPANET 2.0. Since conducting controlled experiments in real WDNs incurs significant challenges, leakage investigation in a laboratory-scale experimental network can serve as a proxy for actual investigation in real networks and deemed more feasible for the model verification process. A realistic network prototype was designed to facilitate leak experimentation and ascertain their impact on the state variables of the system. A stage-wise calibration routine of the base and leak models were undertaken, considering pipe roughness and leak parameters – emitter coefficient and emitter exponent as the unknown variables, respectively. Well-calibrated base and leak models with mean absolute errors of 0.011 and 0.060 were used to assess model performance efficacy and sensitivity analysis of the nodal flow to the nodal pressure and pipe flow in the network.

This study addressed a significant knowledge gap by developing a generalized framework to ascertain the deviation in leakage dynamics in a real WDN model from the theoretical pressure-leak relationship and highlighting the challenges of leakage modeling in real-field models. From the management perspective, an enhanced understanding of the influence of systemic uncertainties on leakage behavior under realistic conditions would be highly beneficial for utility operators and modelers while configuring improved leakage models and strategizing better leakage management protocols. The outcomes of this study may be potentially useful in qualitatively ascertaining the impact of leakage failures on the spatial extent of the WDN and also applicable for generic WDN modeling. The two-stage calibration procedure adopted in this study can be upgraded and implemented in real-time operational networks with physical degradation and leakage.

In future work, the experimental network can be utilized to conduct multi-leak experiments for diverse hydraulic scenarios and investigating the subsequent modeling challenges using hydraulic solvers. A more accurate modeling performance can be attained using multi-objective optimization for model calibration and deriving a more realistic estimation of leak parameters (emitter coefficient and emitter exponent). Diverse methods of setting up the sensitivity matrix and global sensitivity analysis can be conducted to precisely ascertain the local and global leak response. Subsequently, experimentation in the network prototype can be extended to develop and verify model-based leak

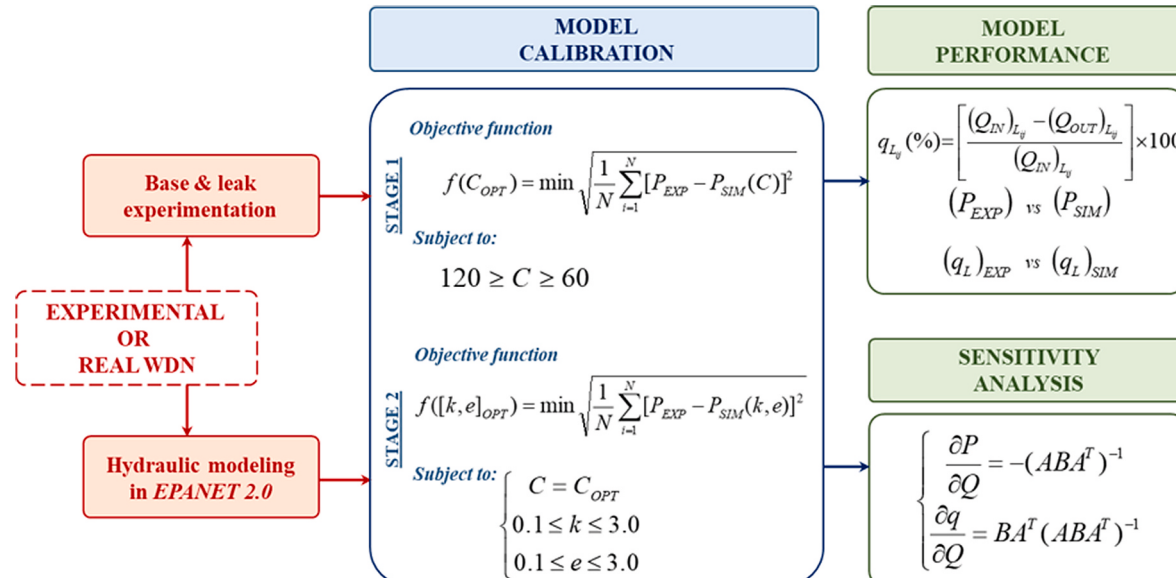


Fig. 11. Overall conceptual framework.

localization and flow rate prediction strategies.

## CRediT authorship contribution statement

**Dina Zaman:** Visualization, experimentation, Formal analysis, Writing – original draft. **Ashok Kumar Gupta:** Conceptualization, Experimentation, Supervision, Writing – review & editing, Resources, Writing – original draft. **Venkatesh Uddameri:** Conceptualization, Writing – review & editing, final draft approval. **Manoj Kumar Tiwari:** Experimentation, Resources, Writing – original draft. **Dhrubajyoti Sen:** Experimentation, Resources, Writing – original draft.

## Declaration of competing interest

The authors declare that they have no known competing financial interests or personal relationships that could have appeared to influence the work reported in this paper.

## Acknowledgments

The authors would like to thank the Ministry of Human Resources and Development (presently, Ministry of Education), Government of India, and Indian Institute of Technology Kharagpur, for funding this research under the mega-project initiative - *Future of Cities*.

## Appendix A. Supplementary data

Supplementary data to this article can be found online at <https://doi.org/10.1016/j.jclepro.2022.132236>.

## References

- Berardi, L., Giustolisi, O., 2021. Calibration of Design Models for Leakage Management of Water Distribution Networks, vols. 1–15. Water Resour. <https://doi.org/10.1007/s11269-021-02847-x>. Manag.
- Bonthuys, G.J., van Dijk, M., Cavazzini, G., 2019. Leveraging water infrastructure asset management for energy recovery and leakage reduction. Sustain. Cities Soc. 46, e101434 <https://doi.org/10.1016/j.scs.2019.101434>.
- Cassa, A.M., van Zyl, J.E., Laubscher, R.F., 2010. A numerical investigation into the effect of pressure holes and cracks in water supply pipes. Urban Water J. 7 (2), 109–120. <https://doi.org/10.1080/15730620903447613>.
- Cassa, A.M., van Zyl, J.E., 2014. Predicting the leakage exponents of elastically deforming cracks in pipes. Procedia Eng. 70, 302–310. <https://doi.org/10.1016/j.proeng.2014.02.034>.
- Cavazzini, G., Pavesi, G., Ardizzone, G., 2020. Optimal assets management of a water distribution network for leakage minimization based on an innovative index. Sustain. Cities Soc. 54, e101890 <https://doi.org/10.1016/j.scs.2019.101890>.
- Chu, S., Zhang, T., Shao, Y., Yu, T., Yao, H., 2020. Numerical approach for water distribution system model calibration through incorporation of multiple stochastic prior distributions. Sci. Total Environ. 708, e134565 <https://doi.org/10.1016/j.scitotenv.2019.134565>.
- Dave, T., Layton, A., 2020. Designing ecologically-inspired robustness into a water distribution network. J. Clean. Prod. 254, e120057 <https://doi.org/10.1016/j.jclepro.2020.120057>.
- Eck, B.J., 2016. An R package for reading EPANET files. Environ. Model. Software 84, 149–154. <https://doi.org/10.1016/j.envsoft.2016.06.027>.
- Eliades, D.G., Kyriakou, M., Vrachimis, S., Polycarpou, M.M., 2016. EPANET-MATLAB toolkit: an open-source software for interfacing EPANET with MATLAB. In: Proc. 14th Int. Conf. Comp. Control. Water. Ind. (CCWI), 8.
- Ferrante, M., 2012. Experimental investigation of the effects of pipe material on the leak head-discharge relationship. J. Hydraul. Eng. 138 (8), 736–743.
- Friedl, F., Möderl, M., Rauch, W., Liu, Q., Schrotter, S., Fuchs-Hanusch, D., 2012. Failure propagation for large-diameter transmission water mains using dynamic failure risk index. In: World Environmental and Water Resources Congress 2012: Crossing Boundaries, pp. 3082–3095. <https://doi.org/10.1061/9780784412312.310>.
- Fox, S., Collins, R., Boxall, J., 2017. Experimental study exploring the interaction of structural and leakage dynamics. J. Hydraul. Eng. 143 (2), e04016080 [https://doi.org/10.1061/\(ASCE\)HY.1943-7900.0001237](https://doi.org/10.1061/(ASCE)HY.1943-7900.0001237).
- Fuchs-Hanusch, D., Steffelbauer, D., Günther, M., Muschalla, D., 2016. Systematic material and crack type specific pipe burst outflow simulations by means of EPANET2. Urban Water J. 13 (2), 108–118. <https://doi.org/10.1080/1573062X.2014.994006>.
- Garnier, M., Holman, I., 2019. Critical review of adaptation measures to reduce the vulnerability of European drinking water resources to the pressures of climate change. Environ. Manag. 64 (2), 138–153. <https://doi.org/10.1007/s00267-019-01184-5>.
- Geng, Z., Hu, X., Han, Y., Zhong, Y., 2019. A novel leakage-detection method based on sensitivity matrix of pipe flow: case study of water distribution systems. J. Water Resour. Plann. Manag. 145 (2), e04018094 [https://doi.org/10.1061/\(ASCE\)WR.1943-5452.0001025](https://doi.org/10.1061/(ASCE)WR.1943-5452.0001025).
- Hu, X., Han, Y., Bin, Y., Geng, Z., Fan, J., 2021. Novel leakage detection and water loss management of urban water supply network using multiscale neural networks. J. Clean. Prod. 278, 123611. <https://doi.org/10.1016/j.jclepro.2020.123611>.
- Ji, L., Wu, T., Xie, Y., Huang, G., Sun, L., 2020. A novel two-stage fuzzy stochastic model for water supply management from a water-energy nexus perspective. J. Clean. Prod. 277, e123386 <https://doi.org/10.1016/j.jclepro.2020.123386>.
- Jun, L., Guoping, Y., 2013. Iterative methodology of pressure-dependent demand based on EPANET for pressure-deficient water distribution analysis. J. Water Resour. Plann. Manag. 139 (1), 34–44. [https://doi.org/10.1061/\(ASCE\)WR.1943-5452.0000227](https://doi.org/10.1061/(ASCE)WR.1943-5452.0000227).
- Koppel, T., Vassiljev, A., 2009. Calibration of a model of an operational water distribution system containing pipes of different age. Adv. Eng. Software 40 (8), 659–664. <https://doi.org/10.1016/j.advengsoft.2008.11.015>.
- Koppel, T., Vassiljev, A., 2012. Use of modelling error dynamics for the calibration of water distribution systems. Adv. Eng. Software 45 (1), 188–196. <https://doi.org/10.1016/j.advengsoft.2011.09.024>.
- Nian-dong, L., Kun, D., Jia-peng, T., Wei-xin, D., 2017. Analytical solution of Jacobian matrices of WDS models. Procedia Eng. 186, 388–396.
- Rossman, L.A., 2000. EPANET 2. User's Manual. US Environmental Protection Agency (EPA), USA.
- Salomons, E., Housh, M., 2020. Practical real-time optimization for energy efficient water distribution systems operation. J. Clean. Prod. 275, e124148 <https://doi.org/10.1016/j.jclepro.2020.124148>.
- Sanjuan-Delmás, D., Petit-Boix, A., Gasol, C.M., Farreny, R., Villalba, G., Suárez-Ojeda, M.E., Gabarrell, X., Josa, A., Riera-deval, J., 2015. Environmental assessment of drinking water transport and distribution network use phase for small to medium-sized municipalities in Spain. J. Clean. Prod. 87, 573–582. <https://doi.org/10.1016/j.jclepro.2014.09.042>.
- Sanz, G., Pérez, R., 2015. Sensitivity analysis for sampling design and demand calibration in water distribution networks using the singular value decomposition. J. Water Resour. Plann. Manag. 141 (10), e04015020 [https://doi.org/10.1061/\(ASCE\)WR.1943-5452.0000035](https://doi.org/10.1061/(ASCE)WR.1943-5452.0000035).
- Schwaller, J., van Zyl, J.V., 2015. Modeling the pressure-leakage response of water distribution systems based on individual leak behavior. J. Hydraul. Eng. 141 (5), e04014089 [https://doi.org/10.1061/\(ASCE\)HY.1943-7900.0000984](https://doi.org/10.1061/(ASCE)HY.1943-7900.0000984).
- Seifollahi-Aghmiuni, S., Haddad, O.B., Omid, M.H., Mariño, M.A., 2013. Effects of pipe roughness uncertainty on water distribution network performance during its operational period. Water Resour. Manag. 27 (5), 1581–1599. <https://doi.org/10.1007/s11269-013-0259-6>.
- Sophocleous, S., Savić, D.A., Kapelan, Z., Giustolisi, O., 2017. A two-stage calibration for detection of leakage hotspots in a real water distribution network. Procedia Eng. 186, 168–176. <https://doi.org/10.1016/j.proeng.2017.03.223>.
- Ssozni, E.N., Reddy, B.D., van Zyl, J.E., 2016. Numerical investigation of the influence of viscoelastic deformation on the pressure-leakage behavior of plastic pipes. J. Hydraul. Eng. 142 (3), e04015057 [https://doi.org/10.1061/\(ASCE\)HY.1943-7900.0001095](https://doi.org/10.1061/(ASCE)HY.1943-7900.0001095).
- Steffelbauer, D., Fuchs-Hanusch, D., 2015. OOPNET: an object-oriented EPANET in Python. Procedia Eng. 119, 710–718. <https://doi.org/10.1016/j.proeng.2015.08.924>.
- Vrachimis, S.G., Timotheou, S., Eliades, D.G., Polycarpou, M.M., 2021. Leakage detection and localization in water distribution systems: a model invalidation approach. Control Eng. Pract. 110, e104755 <https://doi.org/10.1016/j.conengprac.2021.104755>.
- Zaman, D., Tiwari, M.K., Gupta, A.K., Sen, D., 2020. A review of leakage detection strategies for pressurised pipeline in steady-state. Eng. Fail. Anal. 109, e04264 <https://doi.org/10.1016/j.engfailanal.2019.104264>.
- Zaman, D., Tiwari, M.K., Gupta, A.K., Sen, D., 2021a. Performance indicators-based energy sustainability in urban water distribution networks: a state-of-art review and conceptual framework. Sustain. Cities Soc. 72, e103036 <https://doi.org/10.1016/j.scs.2021.103036>.
- Zaman, D., Gupta, A.K., Uddameri, V., Tiwari, M.K., Ghosal, P.S., 2021b. Hydraulic performance benchmarking for effective management of water distribution networks: an innovative composite index-based approach. J. Environ. Manag. 299, e113603 <https://doi.org/10.1016/j.jenvman.2021.113603>.